Cyclic Deformation Behaviors of [$\bar{5}$79]-Oriented Al Single Crystals

PENG LI, SHOUXIN LI, ZHONGGUANG WANG, and ZHEFENG ZHANG

During the cyclic deformation of [$\bar{5}$79], Al single crystals with a high stacking fault energy produced slip bands that were characterized by wavy slip. Its cyclic stress response curve demonstrated that the specimen experienced hardening–softening–secondary hardening in sequence with repeated fluctuation stresses usually less than 10 MPa, which is far lower than those of Cu, Ni, and Ag single crystals. Finally, the whole surface of the Al single crystals was covered with intense intrusion and extrusion, and the cell structure is the most typical dislocation arrangement. These cells mainly comprise loose clusters of dislocations, which move more freely. In the center of the cell, the dislocation density is relatively low, and most dislocations concentrate in the cell wall. At room temperature, compared with cyclically deformed Cu, Ni, and Ag single crystals, the cyclic deformation behaviors of Al single crystals show significant differences, which are highlighted in this study.

DOI: 10.1007/s11661-010-0347-7

I. INTRODUCTION

SINCE Mughrabi[1] established the famous cyclic stress–strain (CSS) curve with three regions for single-slip-oriented Cu single crystal, the cyclic deformation behaviors of various face-centered cubic (fcc) single crystals have been investigated widely. Until now, it is well known that Cu, Ni, and Ag single crystals at room temperature show similar cyclic deformation behaviors, including the formation of a persistent slip bands (PSBs) ladder structure and the appearance of a plateau region.[2–7] Compared with the three typical fcc metals, the cyclic deformation behavior of Al single crystals with a high stacking fault energy (SFE) exhibits more differences, including both the cyclic hardening behavior and dislocation patterns. The related investigations can be retrospected to the 1960s. Snowden[8] and Mitchell and Teer[9,10] successively explored the cyclic hardening curve, surface slip morphology, and microscopic dislocation structure of Al single crystals oriented for single slip. They found that in the earliest stages of fatigue, both striations and matrix formed simultaneously. The matrix in this stage consists of irregular cell boundaries, and the striations crossed these boundaries without apparent interaction. The striations exist prior to the formation of the dipole cluster. At intermediate stages of fatigue, the matrix contained two distinct structures, namely banded loop clusters and cellular regions. With subsequent cyclic deformation, the banded loop structures gradually disappeared, and until the end, the matrix consisted solely of the cellular structure.

PENG LI, Assistant Professor, and SHOUXIN LI, ZHONGGUANG WANG, and ZHEFENG ZHANG, Professors, are with the Shenyang National Laboratory for Materials Science, Institute of Metal Research, Chinese Academy of Sciences, 110016, Shenyang, P.R. China. Contact e-mail: pli@imr.ac.cn
Manuscript submitted March 5, 2010.
Article published online June 26, 2010

The evolution of the dislocation arrangements in fcc single crystals determines the differences in the macroscopic deformation behavior. For cyclic deformation of Al single crystals, a hardening–softening–secondary hardening sequence generally was found. Vorren and Ryum[11] first observed this phenomenon and regarded it as one of the typical features in fatigued Al single crystals. In addition, Vorren and Ryum[12] studied systematically the temperature effect on the cyclic deformation behavior of Al single crystals. They found that at 77 K (–196 °C), mechanical saturation was reached, and the CSS curve had a plateau region in the plastic shear strain amplitude range of $4.2 \times 10^{-3} < \gamma_{pl} < 1.2 \times 10^{-2}$. Furthermore, the dislocation structure formed at 77 K (–196 °C) was rather similar to the two-phase structure developed in Cu single crystals oriented for single slip. Dense bundles of dislocation loops are separated by channels with a much lower dislocation density. But at both room temperature and 77 K (–196 °C), the ladder structure was not observed. However, at 77 K (–196 °C), Charsley and Harris[13] and Charsley *et al.*[14] found that wall structures including PSB-ladder structures appeared in pure polycrystalline Al. Thereafter, Videm and Ryum[15,16] systematically summarized the cyclic deformation behavior of [001] Al single crystals and compared it with the results of polycrystalline Al. They found that highly characteristic deformation patterns with a cord-like appearance at low strain amplitudes and a tweed-like appearance at higher strain amplitudes were developed. The dislocation structure was studied by transmission electron microscopy (TEM) and consisted of {100} dislocation walls and elongated cells. Later, Wang *et al.*[17] studied the variation of stress and dislocation arrangement development in cyclically deformed [001] and [001] Al single crystals. They confirmed that the dislocation arrangement corresponding to [001] crystals developed a wall structure, but in [001] crystals,

the cell structure was still the main dislocation arrangement.

To understand the subsequent fatigue mechanisms of fcc single crystals, it is necessary to abstract the features of the cyclic deformation behavior of Al single crystals and compare them with those of Cu and other fcc metals. The ultimate aim is to find the basic factors controlling the fatigue damage.

II. EXPERIMENTAL PROCEDURES

A bulk Al single crystal plate was grown from electrolytic Al of 99.999 pct purity by the Czochralski method—the crystal orientation of which was determined by electron back-scattering diffraction in a Cambridge S360 scanning electron microscope (SEM) (Cambridge Ltd., Cambridge, England) with accuracy within ±2 deg. Single slip orientation [$\bar{5}79$] was taken as the axially loading direction with a Schmid factor of about 0.406. Then, fatigue specimens of 6 mm × 5 mm × 16 mm in gauge section and 54 mm in total length were made by an electrospark cutting machine. Before fatigue testing, all specimens were electropolished to produce a strain-free and mirror-like surface for microscopic observations. The electrolytic solution for polishing consisted of 50 g anhydrous Mg perchlorate and 450 ml alcohol. The polishing voltage was 12 V with a current of about 6 A.

After the electrolytic polishing, cyclic deformation tests of the specimens were performed under total strain control with a limitation of plastic strain at room temperature in air using a Shimadzu servohydraulic testing machine (Shimadzu Corporation, Kyoto, Japan). A triangular waveform signal with a frequency of 0.5 Hz was used. All specimens were deformed cyclically up to the occurrence of saturation. After fatigue tests, the surface slip morphologies of specimens were observed by a LEO Supra35 SEM (Carl Zeiss International, Oberkochen, Germany). Thin foils for TEM studies were thinned mechanically to ~50 μm thick and then polished by a conventional twin-jet method with a nitric acid solution. The corresponding dislocation arrangements were observed carefully by the Tecnai G2 F30 TEM (FEI Company, Eindhoven, Netherlands). The working current was approximately 50 mA.

III. RESULTS AND DISCUSSION

As shown in Figure 1, the cyclic stress response curve of [$\bar{5}79$] Al single crystals shows a hardening–softening–secondary hardening process with increasing the cyclic number, which is in good agreement with the results from Vorren and Ryum. The cyclic stress response curve is affected slightly by the strain amplitude. At $\gamma_{pl} = 1.23 \times 10^{-3}$, the specimen gradually hardened at first with the increasing cyclic number. When the number of cycles reached about 100, the cyclic deformation entered the saturation stage with a resolved shear stress roughly around 5 MPa. After 1000 cycles, the cyclic hardening occurred again with a continuous

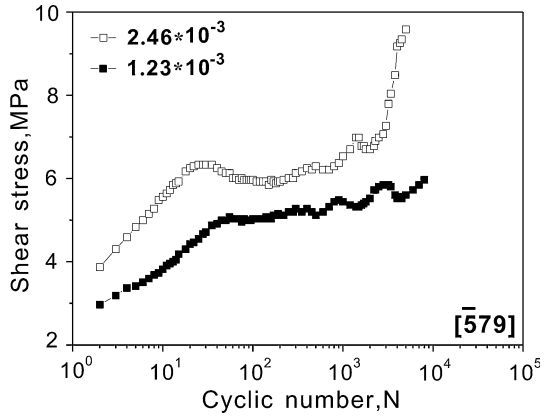

Fig. 1—Cyclic stress response curves of [$\bar{5}79$] Al single crystals at different strain amplitudes.

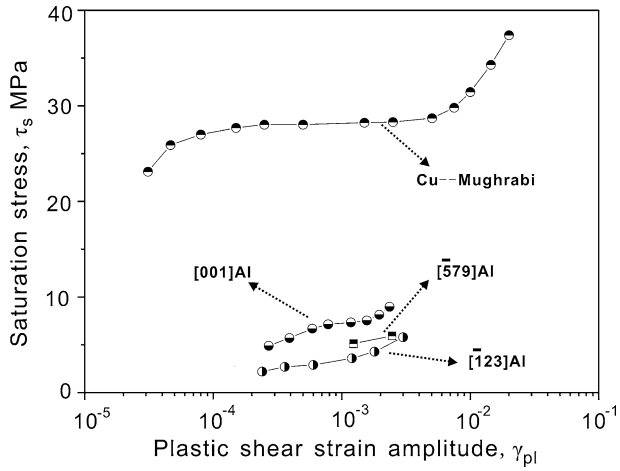

Fig. 2—Comparisons of CSS curves between Cu and Al single crystals. The CSS curve data of Cu single crystals are from Mughrabi[1]; the CSS curve data of [$\bar{1}23$] and [001] Al single crystals are from Videm and Ryum[15] and Vorren and Ryum,[12] respectively.

increase in the stress value. When $\gamma_{pl} = 2.46 \times 10^{-3}$, the cyclic stress response curve exhibited a rapid initial hardening with a stress overshooting stage. Subsequently, a cyclic softening began to occur up to the saturation with a saturation stress of about 6 MPa. Likewise, when the cyclic number is more than 1000, a secondary cyclic hardening appeared. Eventually, the process will be repeated again and again. These observations confirmed that the cyclic saturation of Al single crystals is only an interim behavior. However, in Cu, Ni, and Ag single crystals, the cyclic saturation stage is stable, and the fatigue fracture could not occur at low amplitudes of stress or strain.[1] Besides, a secondary cyclic hardening stage constantly appears in Al single crystals. These experimental results fully demonstrate the unique cyclic stress response characteristic of Al single crystals.

Figure 2 summarized the CSS curves of [$\bar{1}23$], [$\bar{5}79$], and [001] Al single crystals. It should be noted that the saturation stress of Al single crystals is only an approximation because its cyclic stress response curve never has shown a perfect saturation stage similar to

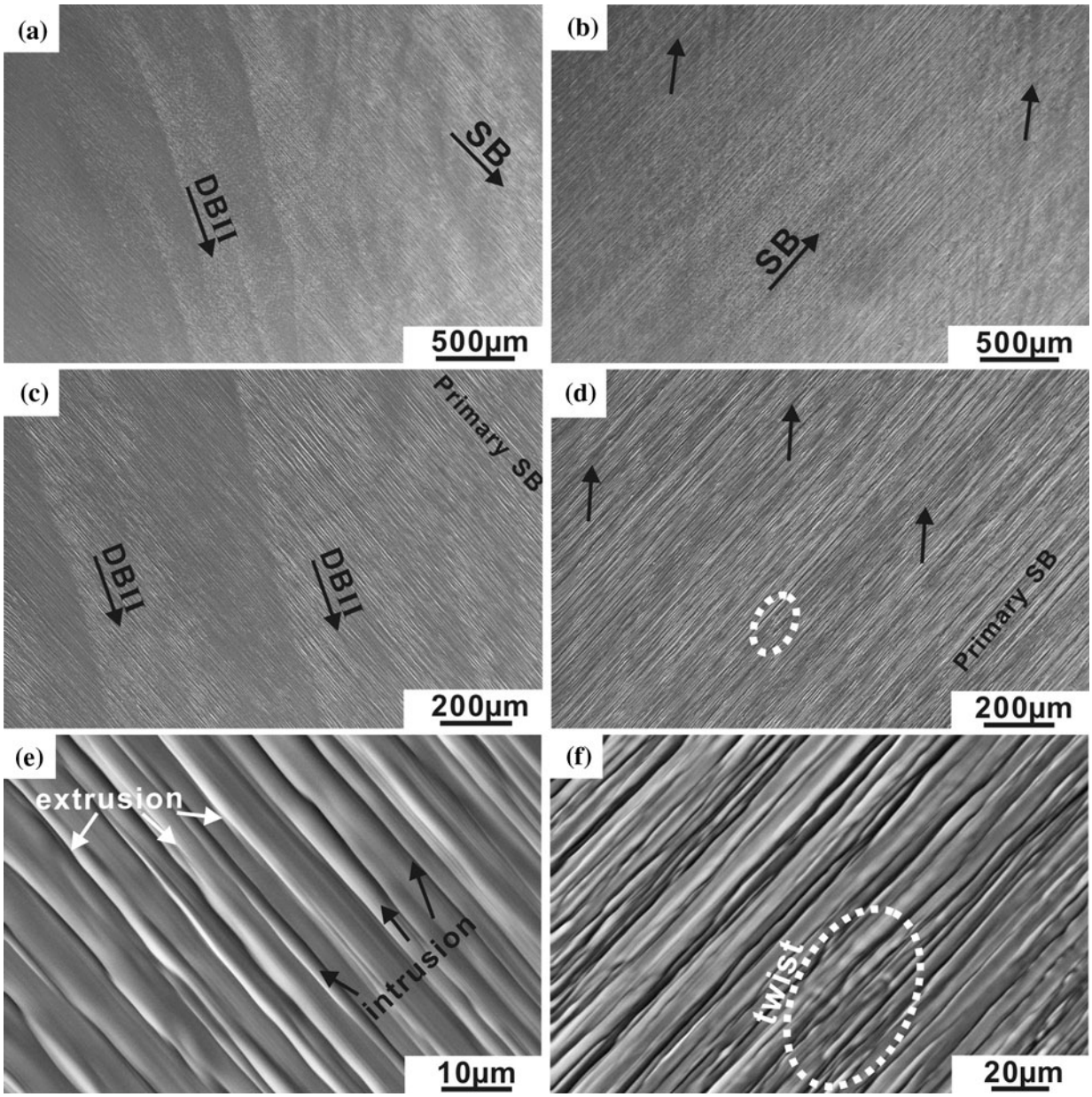

Fig. 3—Surface slip morphologies of [$\bar{5}$79] Al single crystals at different plastic strain amplitudes. (*a*), (*c*), and (*e*) are $\gamma_{pl} = 1.23 \times 10^{-3}$; (*b*), (*d*), and (*f*) are $\gamma_{pl} = 2.46 \times 10^{-3}$. Viewed from the (2$\bar{1}$2) plane.

that of Cu single crystals. Thus, the shear stress followed by the first softening stage (Figure 1) was taken as the saturation stress of Al single crystals in the CSS curve. As shown in Figure 2, the saturation stress of [001] Al single crystals is slightly higher than those of the other two orientations. However compared with that of Cu single crystal, the saturation stresses of all oriented Al single crystals are obviously lower. It is worth noting that the CSS curve of [$\bar{1}$23] Al single crystals seems to show a certain plateau behavior, but on the whole, it is difficult to determine whether the plateau appears in the CSS curves for Al single crystals. However, the cyclic saturation stress of Al single crystals oriented for single slip can be identified roughly as 5 MPa, which basically corresponds to the results reported in previous studies.[11,12]

For [$\bar{5}$79] Al single crystals, the typical slip morphology is shown in Figure 3. Slip bands (SBs) in Al single crystals demonstrate a wavy slip, and the crystal surface is covered with the intense intrusion and extrusion. Figures 3(a), (c), and (e) present the slip morphologies of [$\bar{5}$79] Al single crystals at different magnifications. It is shown that both SBs and deformation band II (DBII) in Al single crystals are similar to those of Cu, Ni, and Ag single crystals,[7,18,19] but the difference is that the slip deformation has saturated in Al single crystals cyclically deformed at high strain amplitudes (Figure 3(d)). In fact, as the strain amplitude increased,

DBII gradually disappeared and was replaced by the local distorted SBs (compared with Figures 3(c) and (d)). These distorted SBs continued to develop and kink bands formed easily. Zhai *et al.*[20] suggested that the formation of a lattice rotation between macrobands and the matrix may be a consequence of the accumulation of the irreversible slip. According to the current investigations, the formation of the twist will contribute to the occurrence of secondary cyclic hardening in fatigued Al single crystals, leading to the obvious fluctuation of a cyclic hardening curve (see Figure 3(d)). Videm and Ryum[15,16] observed the similar slip morphologies in [001] Al single crystals at low strain amplitudes and referred to them as the cord-like structures. As shown in Figures 3(b), (d), and (f), cord-like structures are one of the classic morphologies in fatigued Al single crystals. Early in the cycling process, the cord structure did not cover the entire surface. With subsequent cyclic deformation, they finally covered the entire surface.[15] Videm *et al.*[15] suggested that when crystals were cycled at $\varepsilon \geq 4.8\times10^{-4}$, the tweed-like pattern built up without the preceding formation of the cord structure, but it was formed by narrow lines at ±45 deg with respect to the loading axis. In this experiment, despite the applied high strain amplitude, the cyclic number is still not enough to form the tweed-like structure. In Al single crystals, deformation patterns generally include cord-like structure, tweed-like structure, and macrobands consisting of SBs.

In addition to the surface morphology, the microscopic dislocation structure of fatigued Al single crystals is of particular interest. Figure 4 exhibits the typical dislocation arrangements of single-slip-oriented Al single crystals, including $\bar{5}79$ in the current work and $[\bar{1}25]$ from Zhai *et al.*[21] Dislocation cells are the most classic dislocation arrangements in both $[\bar{5}79]$ and $[\bar{1}25]$ Al single crystals induced by cyclical deformation. The clusters comprising plenty of dislocation loops were distributed along these cell walls. The center of these cells only contains a relatively low density of dislocations, and most dislocations concentrate in the cell wall, which is shown clearly when comparing Figures 4(b) and (e). Grosskreutz and Waldow[22] attributed the formation of these cells to a fatigue-induced substructure. Here, we just considered that the formation of cells is related directly to the appearance of intense SBs and the occurrence of the secondary cyclic hardening behavior. For Al single crystals, the SFE is high, and cross slip continually occurs during cyclic deformation. Thus, it is almost impossible for the dislocations to be trapped with each other or massed. As shown in Figures 4(c) and (f), the dislocations in the cell are looser than those in PSB ladders, and the dislocation movement has a greater freedom; thus, the dislocations will not be bound easily to a place. On the other hand, because of the larger freedom of dislocation movement in Al single crystals, a nonprimary slip system will be activated more easily during cyclic deformation. The activation of the secondary slip system plus the lattice rotation brings some accumulation points in Al single crystals.[20] To some extent, these accumulation points contribute to the dislocation concentration. And then the cell structure

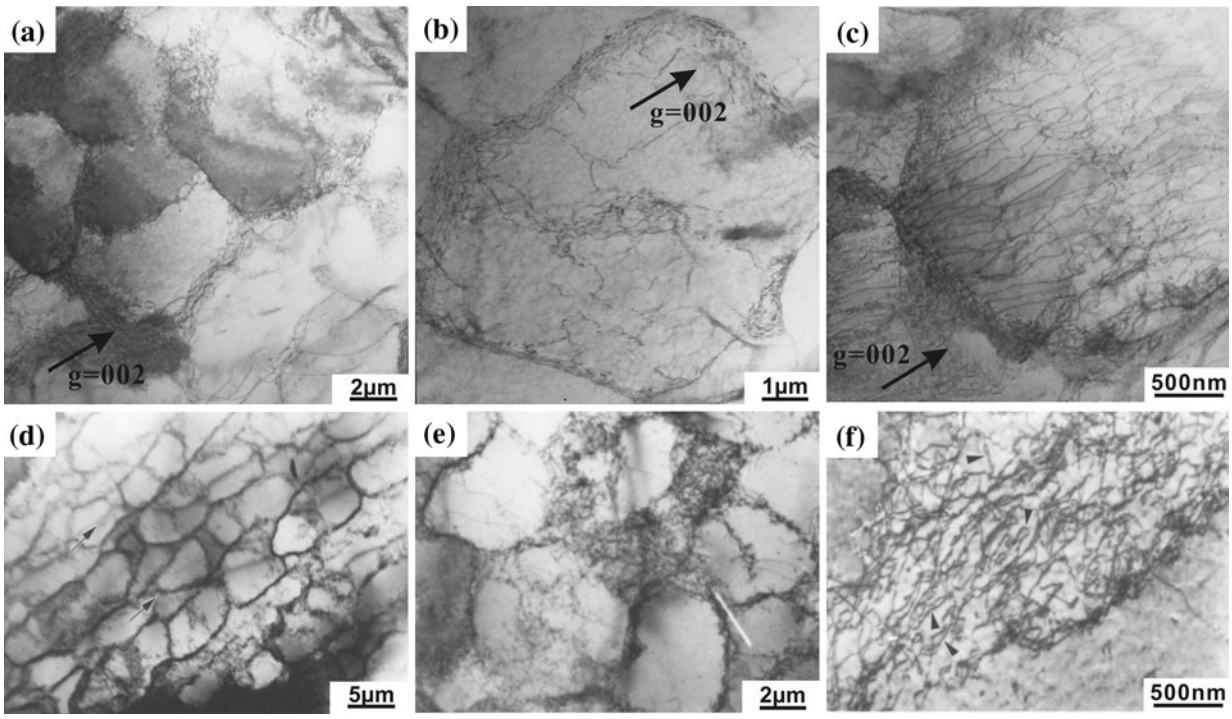

Fig. 4—Dislocation patterns of differently oriented Al single crystals. (*a*) through (*c*) are $[\bar{5}79]$ Al single crystals at the strain amplitude $\gamma_{pl} = 2.46 \times 10^{-3}$ and the foil $\|(110)$; (*d*) through (*f*) are $[\bar{1}25]$ Al single crystals at the constant resolved shear stress amplitude of 4 MPa and the foil $\|(1\bar{2}1)$. The $[\bar{1}25]$ Al single crystals come from Zhai *et al.*[21]

finally forms under the action of a cross slip of screw dislocations. The formation of the cell structure corresponds to the appearance of intense SBs on the surface. The easy activation of the secondary slip system results in the secondary cyclic hardening of Al single crystals.

As early as the 1950s, Segall and Partridge[23] pointed out qualitatively that at a high stress amplitude (given a life of 10^5 cycles), the cell structure would form in fatigued Al single crystals. However, at a low stress amplitude (given a life greater than 10^6 cycles), the dislocations were distributed randomly, and the cell structure did not appear. Based on plenty of previous results and the current research, the cell structure is seen most commonly in Al single crystals with various orientations, including single-slip orientations [$\bar{1}$23], [$\bar{1}$25], and [$\bar{5}$79][9,10,12,20,21,24,25]; double-slip orientations [$\bar{1}$12], [$\bar{1}$14], and [$\bar{1}$120][26]; and even multiple-slip orientations [001] and [011].[15–17] In other words, whether the cell forms is not dominated by the orientation of Al single crystals but is determined by the characteristic of Al itself.

Briefly, compared with Cu, Ni, and Ag single crystals,[27] the most remarkable feature of Al single crystals is that the SFE is much higher than those of the three fcc metals. Although it is generally accepted that the aforementioned fcc metals are classified as wavy slip materials, the slip mode of these fcc metals will not be exactly the same because of the difference in their SFE, which mainly is related to the ease or difficulty of cross slip. It needs to be emphasized that the SFE is not the only important factor, and the effect of testing temperature should not be ignored. The related research on the cyclic deformation behaviors of Cu single crystals at various temperatures were accomplished by Basinski *et al.*,[28–31] Lisiecki and Weertman,[32,33] Boehme *et al.*,[34] and Buchinger *et al.*[35] Similarly, the effect of temperature on the fatigue behavior of Ni single crystals also is investigated further. Bretschneider and Holste[4,36,37] summarized the typical fatigue behaviors of an Ni single crystal with single-slip orientation when the testing temperature was changed between 77 K (–196 °C) to 900 K (627 °C). They suggested that the CSS curve of Ni single crystals fatigued in this temperature range still showed the plateau behavior, but both the plateau stresses and the plastic strain amplitudes at the upper and the lower borders of these plateaus decreased with an increasing temperature, which was similar to those of Cu single crystals. Room temperature for Al is a relatively higher temperature than for the other fcc metals. Charsley *et al.*[13,14] investigated the cyclic deformation behaviors of pure polycrystalline Al in the total strain amplitude range of 2×10^{-4} to 1.4×10^{-3} at temperatures of 77 K (–196 °C), 163 K (–110 °C), and 223 K (–50 °C). They found that wall structures including PSB-ladder structures could be observed only within limited ranges of temperature and strain amplitude. Therefore, when the formation mechanism of dislocation arrangements is investigated, it is also necessary to consider the combined effect of SFE with the testing temperature, which also will be the core issue to be discussed in future.[38]

IV. CONCLUSIONS

1. The cyclic stress response curve of [$\bar{5}$79] Al single crystals shows a hardening–softening–secondary hardening feature. By comparing the CSS curves of differently oriented Al single crystals, it was found that the saturation stress of [001] Al single crystals corresponding to the softening stage is slightly higher than those of [$\bar{1}$23] and [$\bar{5}$79] single crystals. However, the saturation stress of Al single crystals with orientations including [001], [$\bar{1}$23], and [$\bar{5}$79] is only about 5 MPa to 6 MPa, which is much lower than that of Cu single crystals oriented for single slip. However, unlike Cu single crystals, Al single crystals do not show an obvious plateau behavior in its CSS curves.
2. In Al single crystals, SBs show a wavy slip, and the crystal surface is covered with the intense intrusion and extrusion. At low strain amplitude, DBII appears in Al single crystals, which is similar to those of Cu and Ni single crystals. At a higher strain amplitude, SBs clustered in macrobands becomes the major slip morphology. The formation of such morphology is related closely to the secondary hardening behavior. Furthermore, it is confirmed that the appearance of intense SBs is a result of the formation of a cell structure in fatigue Al single crystals. For Al single crystals, no matter what the orientation is, the dislocation arrangements are basically cell structure. In the center of the cell, the dislocation density is relatively low, and most dislocations concentrate in the cell wall. The cell walls consist of loose dislocation loops; thus, the dislocation movement has a greater freedom than that in Cu, Ni, or Ag crystals.

ACKNOWLEDGMENTS

The authors are grateful to S.D. Wu, H.H. Su, W. Gao, L.X. Zhang, J.L. Wen, and H.F. Zou for their assistance in the sample preparation, fatigue experiments, and dislocation observations. This work was supported financially by the "Hundred of Talents Project" of Chinese Academy of Sciences, the National Outstanding Young Scientist Foundation under Grant No. 50625103, and the National Basic Research Program of China under Grant No. 2010CB631006.

REFERENCES

1. H. Mughrabi: *Mater. Sci. Eng.*, 1978, vol. 33, pp. 207–23.
2. H. Mughrabi, F. Ackermann, and K. Herz: in *Fatigue Mechanisms*. ASTM STP 675, J.T. Fong, ed., ASTM, Philadelphia, 1979, pp. 69–105.
3. A.T. Winter: *Philos. Mag.*, 1974, vol. 30, pp. 719–38.
4. J. Bretschneider, C. Holste, and B. Tippelt: *Acta Mater.*, 1997, vol. 45, pp. 3775–83.
5. P. Li, Z.F. Zhang, S.X. Li, and Z.G. Wang: *Acta Mater.*, 2008, vol. 56, pp. 2212–22.
6. P. Li, Z.F. Zhang, S.X. Li, and Z.G. Wang: *Scripta Mater.*, 2008, vol. 59, pp. 730–33.
7. P. Li, Z.F. Zhang, X.W. Li, S.X. Li, and Z.G. Wang: *Acta Mater.*, 2009, vol. 57, pp. 4845–54.

8. K.U. Snowden: *Acta Metall.*, 1963, vol. 11, pp. 675–84.
9. A.B. Mitchell and D.G. Teer: *Philos. Mag.*, 1969, vol. 19, pp. 609–12.
10. A.B. Mitchell and D.G. Teer: *Philos. Mag.*, 1970, vol. 22, pp. 399–417.
11. O. Vorren and N. Ryum: *Acta Metall.*, 1988, vol. 36, pp. 1443–53.
12. O. Vorren and N. Ryum: *Acta Metall.*, 1987, vol. 35, pp. 855–66.
13. P. Charsley and L.J. Harris: *Scripta Metall.*, 1987, vol. 21, pp. 341–44.
14. P. Charsley, U. Bangert, and L.J. Appleby: *Mater. Sci. Eng. A*, 1989, vol. 113, pp. 231–36.
15. M. Videm and N. Ryum: *Mater. Sci. Eng. A*, 1996, vol. 219, pp. 1–10.
16. M. Videm and N. Ryum: *Mater. Sci. Eng. A*, 1996, vol. 219, pp. 11–20.
17. J. Wang, Z.G. Zhu, Q.F. Fang, and G.D. Liu: *Mater. Res. Bull.*, 1999, vol. 34, pp. 407–13.
18. Z.F. Zhang, Z.G. Wang, and Z.M. Sun: *Acta Mater.*, 2001, vol. 49, pp. 2875–86.
19. C. Buque: *Int. J. Fatigue*, 2001, vol. 23, pp. 671–78.
20. T. Zhai, J.W. Martin, G.A.D. Briggs, and A.J. Wilkinson: *Acta Mater.*, 1996, vol. 44, pp. 3477–88.
21. T. Zhai, J.W. Martin, and G.A.D. Briggs: *Acta Mater.*, 1996, vol. 44, pp. 1729–39.
22. J.C. Grosskreutz and P. Waldow: *Acta Metall.*, 1963, vol. 11, pp. 717–24.
23. R.L. Segall and P.G. Partridge: *Philos. Mag.*, 1959, vol. 4, pp. 912–19.
24. T. Zhai, J.W. Martin, and G.A.D. Briggs: *Acta Metall. Mater.*, 1995, vol. 43, pp. 3813–25.
25. T. Zhai, G.A.D. Briggs, and J.W. Martin: *Acta Mater.*, 1996, vol. 44, pp. 3489–96.
26. T. Fujii, N. Sawatari, S. Onaka, and M. Kato: *Mater. Sci. Eng. A*, 2004, vols. 387–389, pp. 486–90.
27. Z.R. Wang: *Philos. Mag.*, 2004, vol. 84, pp. 351–79.
28. Z.S. Basinski, A.S. Korbel, and S.J. Basinski: *Acta Metall.*, 1980, vol. 28, pp. 191–207.
29. Z.S. Basinski and S.J. Basinski: *Acta Metall.*, 1989, vol. 37, pp. 3255–62.
30. Z.S. Basinski and S.J. Basinski: *Acta Metall.*, 1989, vol. 37, pp. 3263–73.
31. Z.S. Basinski and S.J. Basinski: *Prog. Mater. Sci.*, 1992, vol. 36, pp. 89–148.
32. L.L. Lisiecki and J.R. Weertman: *Scripta Metall.*, 1986, vol. 20, pp. 249–52.
33. L.L. Lisiecki and J.R. Weertman: *Acta Metall. Mater.*, 1990, vol. 38, pp. 509–19.
34. F. Boehme, K. Hidaka, and J.R. Weertman: *Scripta Metall. Mater.*, 1990, vol. 24, pp. 2341–46.
35. L. Buchinger, S. Stanzl, and C. Laird: *Philos. Mag. A*, 1990, vol. 62, pp. 633–51.
36. J. Bretschneider, C. Holste, and W. Kleinert: *Mater. Sci. Eng. A*, 1995, vol. 191, pp. 61–72.
37. A. Schwab, J. Bretschneider, C. Buque, C. Blochwitz, and C. Holste: *Philos. Mag. Lett.*, 1996, vol. 74, pp. 449–54.
38. P. Li, S.X. Li, Z.G. Wang, and Z.F. Zhang: *Prog. Mater. Sci.*, in press.